



Role for ribosome-associated quality control in sampling proteins for MHC class I-mediated antigen presentation

Débora Broch Trentini^a, Matteo Pecoraro^b, Shivani Tiwary^c, Jürgen Cox^{c,d}, Matthias Mann^b, Mark S. Hipp^{a,1,2}, and F. Ulrich Hartl^{a,2}

^aDepartment of Cellular Biochemistry, Max Planck Institute of Biochemistry, 82152 Martinsried, Germany; ^bDepartment of Proteomics and Signal Transduction, Max Planck Institute of Biochemistry, 82152 Martinsried, Germany; ^cComputational Systems Biochemistry Research Group, Max Planck Institute of Biochemistry, 82152 Martinsried, Germany; and ^dDepartment of Biological and Medical Psychology, University of Bergen, 5009 Bergen, Norway

Edited by Alexander Varshavsky, California Institute of Technology, Pasadena, CA, and approved January 20, 2020 (received for review August 21, 2019)

Mammalian cells present a fingerprint of their proteome to the adaptive immune system through the display of endogenous peptides on MHC-I complexes. MHC-I-bound peptides originate from protein degradation by the proteasome, suggesting that stably folded, long-lived proteins could evade monitoring. Here, we investigate the role in antigen presentation of the ribosome-associated quality control (RQC) pathway for the degradation of nascent polypeptides that are encoded by defective messenger RNAs and undergo stalling at the ribosome during translation. We find that degradation of model proteins by RQC results in efficient MHC-I presentation, independent of their intrinsic folding properties. Quantitative profiling of MHC-I peptides in wild-type and RQC-deficient cells by mass spectrometry showed that RQC substantially contributes to the composition of the immunopeptidome. Our results also identify endogenous substrates of the RQC pathway in human cells and provide insight into common principles causing ribosome stalling under physiological conditions.

ribosome-associated quality control | Listerin | MHC-I | immunopeptidome

The major histocompatibility complex (MHC) molecules play a central role in the vertebrate adaptive immune system. MHC class I binds to short peptides (8 to 11 amino acids long) sampled from the proteolytic products of intracellular proteins. MHC-I-loaded peptides are presented at the cell surface, where they are surveyed by CD8⁺ T cells for the presence of non-self-peptides (1). This system, present in all nucleated cells of higher vertebrates, enables the recognition of cells infected with viruses and other intracellular parasites, or cells accumulating aberrant proteins resulting from malignant transformation. The presented peptides originate mostly from degradation by the ubiquitin-proteasome system (2, 3), which is responsible for the controlled turnover of the great majority of cellular proteins, and for the rapid degradation of defective species (4). The immune response is remarkably efficient. In cultured cells, CD8⁺ T cells can recognize infected cells in less than 60 min after viral penetration (5), despite the fact that viral proteins are usually very stable and have slow turnover rates (6). Accordingly, cells require a mechanism for rapidly generating peptides from long-lived viral proteins synthesized upon infection.

To explain the kinetic discrepancy between protein half-life and MHC-I presentation, defective ribosomal products (DRiPs) have been proposed to act as a significant source of self-peptides and viral peptides. DRiPs were defined as proteins that do not reach mature (stable) conformation and, unable to fold or assemble correctly, are targeted for rapid proteasomal degradation (7). The DRiP designation later evolved to include errors in transcription, splicing, and translation (8). While estimates for the fraction of rapidly degraded newly synthesized proteins varied considerably (6, 9–13), it has also been suggested that proteasome substrates differ in their access to MHC-I presentation, with “true DRiPs” undergoing privileged processing for presentation (14, 15). Therefore, one appealing notion of the DRiP hypothesis is

that production of an antigenic peptide would depend largely on the rate of translation of the corresponding protein, and less on its relative abundance or turnover once folded and assembled. This would be particularly important for viral proteins, which constitute only a minute fraction of the total cellular pool of proteins at the early stages of infection (7). A number of studies showed that presentation of certain model proteins is inefficient in the absence of active synthesis, despite the presence of a large pool of mature forms being degraded (16–18), while others reported productive presentation of mature proteins (19, 20). The mechanism of DRiP generation and the overall contribution of DRiPs to antigen presentation remain areas of active research.

Here, we test the hypothesis that the ribosome-associated quality control (RQC) machinery may play a role in MHC-I antigen presentation. RQC is a conserved eukaryotic pathway

Significance

Pathogens and tumors are detected by the immune system through the display of intracellular peptides on MHC-I complexes. These peptides are generated by the ubiquitin-proteasome system preferentially from newly synthesized polypeptides. Here we show that the ribosome-associated quality control (RQC) pathway, responsible for proteasomal degradation of polypeptide chains that stall during translation, mediates efficient antigen presentation of model proteins independent of their intrinsic folding properties. Immunopeptidome characterization of RQC-deficient cells shows that RQC contributes to the presentation of a wide variety of proteins, including proteins that may otherwise evade presentation due to efficient folding. By identifying endogenous substrates of the RQC pathway in human cells, our results also enable the analysis of common principles causing ribosome stalling under physiological conditions.

Author contributions: D.B.T., M.M., M.S.H., and F.U.H. designed research; D.B.T., M.P., and S.T. performed research; D.B.T., M.P., S.T., J.C., M.M., M.S.H., and F.U.H. analyzed data; and D.B.T., M.S.H., and F.U.H. wrote the paper.

The authors declare no competing interest.

This article is a PNAS Direct Submission.

This open access article is distributed under [Creative Commons Attribution-NonCommercial-NoDerivatives License 4.0 \(CC BY-NC-ND\)](https://creativecommons.org/licenses/by-nc-nd/4.0/).

Data deposition: The mass spectrometry proteomics data have been deposited to the ProteomeXchange Consortium via the PRIDE partner repository with the dataset identifier [PXD014644](https://doi.org/10.1093/bioinformatics/btq014).

¹Present addresses: Department of Biomedical Sciences of Cells and Systems, University Medical Center Groningen, University of Groningen, 9713 AV Groningen, The Netherlands; and School of Medicine and Health Sciences, Carl von Ossietzky University Oldenburg, 26111 Oldenburg, Germany.

²To whom correspondence may be addressed. Email: m.s.hipp@umcg.nl or uhartl@biochem.mpg.de.

This article contains supporting information online at <https://www.pnas.org/lookup/suppl/doi:10.1073/pnas.1914401117/-DCSupplemental>.

First published February 11, 2020.

that removes nascent polypeptide chains from ribosomes that have stalled during translation (21) and thus qualify as DRiPs. In contrast to quality control mechanisms that monitor the folding state of newly synthesized polypeptides, RQC senses the state of translation (22). RQC comprises five steps: sensing of elongation stalling, ribosome splitting and messenger RNA (mRNA) dissociation, assembly of the RQC machinery on the 60S subunit, ubiquitylation of the nascent chain, and its extraction for proteasomal degradation. The core components of the RQC machinery in mammals are the ubiquitin ligase Listerin (23) and the factors NEMF and TCF25 (respectively, Ltn1/Rqc2/Rqc1 in yeast) (21, 22, 24). NEMF/Rqc2 recognizes the peptidyl-transfer RNA moiety at the interface of the dissociated 60S ribosome and recruits Listerin/Ltn1 (24, 25), which mediates ubiquitylation of the stalled polypeptide near the ribosome exit tunnel (25–27). RQC is intimately linked to two mRNA degradation pathways that take place in the cytoplasm: nonstop mRNA decay (28) and no-go decay (29), which recognize mRNAs that lack stop codons and mRNAs that present obstacles to elongation, respectively. The resulting nascent protein is truncated and/or mutated and therefore likely to be dysfunctional, but not necessarily misfolded. The RQC pathway ensures that these aberrant species are committed to degradation. Although it evolved earlier than the adaptive immune system, the RQC pathway has many appealing characteristics for a coopted function in MHC-I antigen presentation. RQC-mediated degradation is comprehensive, as stalling can occur for mRNAs of any gene. In addition, it is folding-unbiased, as, according to current understanding, the mRNA properties are critical for RQC recruitment and not the folding state of the nascent chain. Finally, in line with the DRiP hypothesis, degradation by the RQC machinery acts on actively translated proteins rather than the existing protein pool.

Here we used model proteins to show that the RQC machinery generates antigenic peptides from nascent chains encoded by defective mRNA molecules, and that folding to a stable structure does not allow nascent chains to escape from RQC-mediated presentation. Furthermore, we assess the contribution of RQC degradation to antigen presentation under normal growth conditions by profiling the MHC-I-bound peptidome of wild-type (WT) and Listerin knockout (KO) cells by mass spectrometry (MS). The results demonstrate that RQC degradation substantially influences the composition of the immunopeptidome. Our analysis also provides a dataset of natural RQC degradation substrates in human cells, providing insights into this still largely uncharacterized degradation pathway.

Results

Characterization of Model Proteins for RQC-Mediated Antigen Presentation. To assess the potential of the RQC pathway to generate antigenic peptides, we designed model proteins that can be directed to either RQC-mediated or misfolding-induced degradation. To this end, we employed destabilizing domains (DDs), small protein domains designed to be unfolded and rapidly degraded but stabilized in the presence of a cell-permeable ligand (30, 31) (Fig. 1A), thus allowing control of folding status. The FKBP_{DD} (32) and the DHFR_{DD} (33) DDs, responsive to the Shield1 and trimethoprim ligands, respectively, were fused to the antigenic peptide SIINFEKL and eGFP (Fig. 1A). The SIINFEKL sequence from ovalbumin allows us to monitor presentation using the well-characterized monoclonal antibody mAb 25-D1.16 (34), which specifically recognizes SIINFEKL-bound murine MHC-I complex H-2K^b. To create versions of these constructs directed to RQC degradation, we removed the stop codons of the respective genes (Fig. 1A). Expression of the nonstop (NS) model proteins results in translation into the 3'UTR and polyadenylation tail, the latter causing ribosomes to stall (35, 36). The DD-SIINFEKL-GFP STOP and NS fusion proteins were introduced into the HeLa.K^b cell line (37) that stably expresses the mouse H-2K^b MHC-I protein.

Experiments were performed using stable monoclonal cell lines for each construct in WT and in RQC-deficient (Listerin-KO) cells obtained by CRISPR/Cas (*SI Appendix, Fig. S1*). Cycloheximide (CHX) chase experiments confirmed that both DD fusions (STOP versions) were stable in the presence of ligand (half-life of >9 h), but rapidly degraded in the absence of ligand, with a half-life of ~4 h for FKBP STOP and ~30 min for DHFR STOP (Fig. 1B). Thus the FKBP_{DD} and DHFR_{DD} of the fusion proteins fold independently of the SIINFEKL-eGFP and are stabilized by the respective ligand.

Next, we compared the effect of DD ligand and the proteasome inhibitor MG132 on protein levels. Addition of ligand for 4 h increased GFP levels approximately fivefold for the STOP proteins and approximately twofold for the NS proteins (Fig. 1C). Combining DD ligand with MG132 did not result in a further stabilization of the STOP proteins, but rather decreased their level by ~20%, as overall protein synthesis slowed after 1 h of proteasome inhibition (38) (Fig. 1C and *SI Appendix, Fig. S2*). In contrast, NS protein GFP levels increased ~18-fold upon combined treatment with DD ligand and MG132 (Fig. 1C). Thus, for the NS proteins, the majority of degradation is independent of the fold stabilizing effect of ligand on their N-terminal domains, in contrast to the turnover of the STOP proteins.

We next analyzed the effect of Listerin on protein levels. As expected, deletion of Listerin was essentially without effect on the levels of the STOP constructs (Fig. 1C). In contrast, the steady-state levels of the NS proteins increased approximately fivefold in the absence of Listerin (Fig. 1C). Notably, proteasome inhibition further enhanced the levels of NS proteins (Fig. 1C). This finding indicates that Listerin is not the only E3 ubiquitin ligase that mediates NS protein degradation in human cells, consistent with a recent report that, in yeast, the E3 ubiquitin ligase Hul5 can mediate degradation of RQC substrates that escape ubiquitylation by Ltn1 (39).

Degradation by RQC Results in Robust Antigen Presentation. To compare the rate of antigen presentation of STOP and NS proteins, we performed a kinetic analysis of FKBP and DHFR presentation in the HeLa.K^b WT background in the absence and presence of DD ligand. Cells were stripped of surface antigens by acid wash (40), and the appearance of MHC-I-bound SIINFEKL peptide on the cell surface was monitored by antibody labeling and flow cytometry. Total protein synthesis was concomitantly determined by measuring intracellular GFP fluorescence after blocking protein degradation with MG132 plus stabilizing ligand.

Presentation of the NS proteins in absolute terms was lower than that of the respective STOP proteins, consistent with the lower levels of NS protein being produced (Fig. 2A), as NS mRNAs are sensed as defective and undergo silencing and/or degradation (28, 41). We therefore normalized the presentation rate in the linear range of the assay (1 to 3 h) to the rate of expression. The latter was estimated as the slope of GFP fluorescence in the presence of MG132 and DD ligand between 0 and 1 h of culturing (Fig. 2B) to avoid stress-induced translational shutdown due to proteasome inhibition (*SI Appendix, Fig. S2*). Ligand-induced fold stabilization substantially reduced presentation for the STOP proteins, but did not significantly affect presentation of the NS proteins (Fig. 2C). In the absence of ligand, the expression-normalized presentation of NS proteins can be similar to (DHFR) or even approximately threefold higher (FKBP) than presentation of the respective STOP proteins (Fig. 2C). Note that this difference in relative presentation is due to the approximately fivefold-higher presentation of DHFR STOP than FKBP STOP ($P = 0.0002$) in the absence of ligand, which is consistent with the lower half-life of the DHFR_{DD} construct (Fig. 1B). Strikingly, in the presence of ligand, the normalized presentation rate of both NS proteins was substantially higher than that of the respective STOP proteins: sixfold for FKBP and twofold for DHFR (Fig. 2C). Of note is that

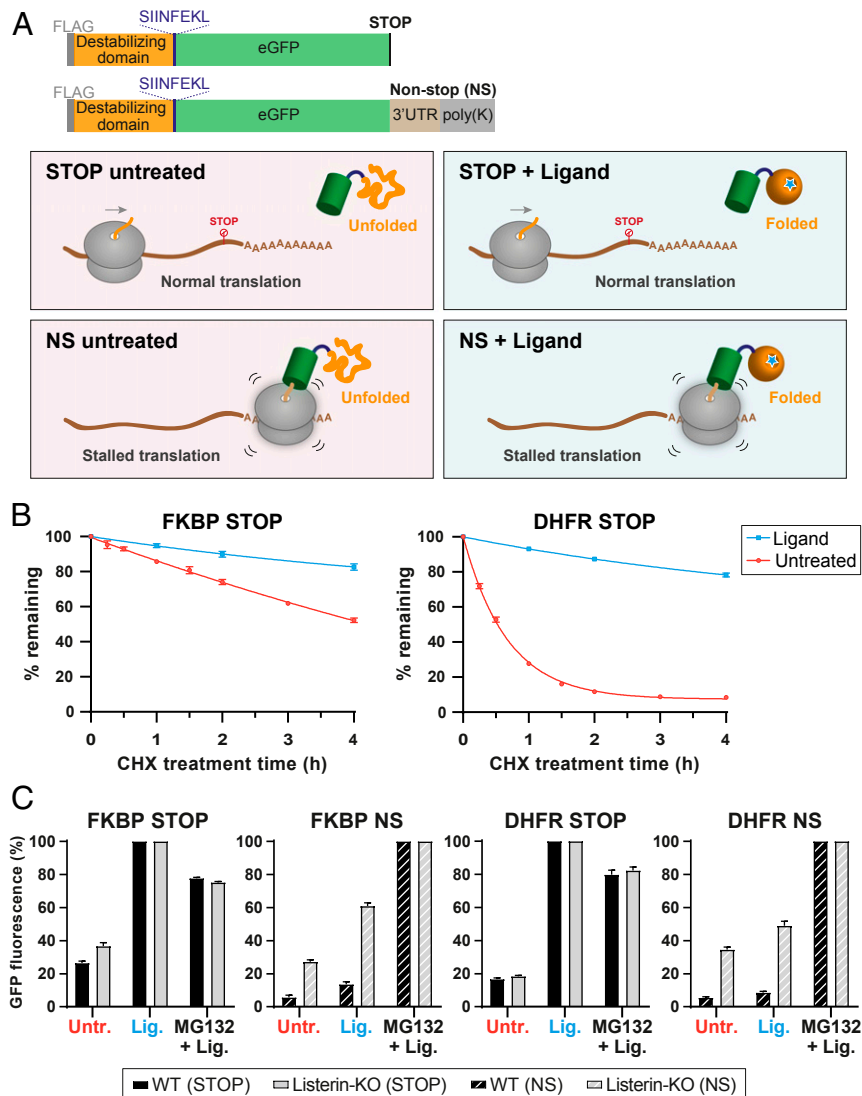


Fig. 1. Model STOP and NS constructs. (A) (Top) Model constructs used in this study. DDs, FKBP_{DD} or DHFR_{DD}, were fused to the antigenic peptide SIINFEKL and eGFP. Each construct was created in two versions, STOP (normal translation termination) and NS, where translation proceeds into the 3'UTR and poly(A) tail (encoding a polyK chain), resulting in ribosome stalling. (Bottom) Scheme depicting predicted effects of ligands on STOP and NS proteins. (B) Protein stability of STOP constructs in the presence or absence of DD ligand, as measured by monitoring GFP fluorescence after inhibition of protein synthesis with CHX. (C) Response of STOP and NS constructs (GFP fluorescence levels) to stabilizing ligand and proteasome inhibitor MG132 in WT and Listerin-KO cells. To facilitate comparison, values are normalized to the maximum intensity obtained for the respective construct (ligand for STOP proteins, MG132+ligand for NS proteins). In B and C, graphs show the average of three independent experiments, and error bars indicate SD.

addition of ligand did not completely abrogate presentation of STOP proteins, an observation we attribute to the small but detectable turnover of stably folded protein (Fig. 1B) and the likely possibility that a small fraction of the newly synthesized STOP proteins will form defective species, in line with the DRiP hypothesis. The highly efficient presentation of the NS proteins compared to the basal level of STOP protein presentation (in the presence of ligand) indicates that RQC represents a fast and robust way to sample folding-efficient proteins. Thus, for proteins that would otherwise evade degradation due to optimized folding, as is often the case for viral proteins, the RQC pathway may provide an effective mechanism for presentation.

To confirm the role of Listerin in NS protein presentation, we expressed the NS fusion constructs in WT and Listerin-KO HeLa.K^b cells, as well as in stably complemented Listerin-KO cells (cKO). As expected, Listerin-KO cells had significantly higher levels of NS proteins than Listerin-expressing cells (Fig. 3

and *SI Appendix*, Fig. S3). Conversely, presentation was significantly higher in the Listerin-expressing cells (Fig. 3 and *SI Appendix*, Fig. S3). Interestingly, neither degradation nor presentation of the NS proteins was completely abolished in the Listerin-KO cells (Fig. 3), consistent with the presence of an E3 ligase component(s) functionally redundant to Listerin. Thus, the observed difference in presentation between WT and Listerin-KO cells is likely to underestimate the total contribution of the RQC pathway to NS protein presentation.

Global Analysis of Listerin-Dependent Antigen Presentation. To investigate how RQC degradation affects the MHC-I peptide repertoire, we compared the immunopeptidome of WT and Listerin-KO HeLa.K^b cells. To quantitatively profile the MHC-I-bound peptides, MHC-I immunoprecipitations were performed from six independent cultures of WT and Listerin-KO cells, and from two cultures of cKO cells, followed by immunopeptide elution and

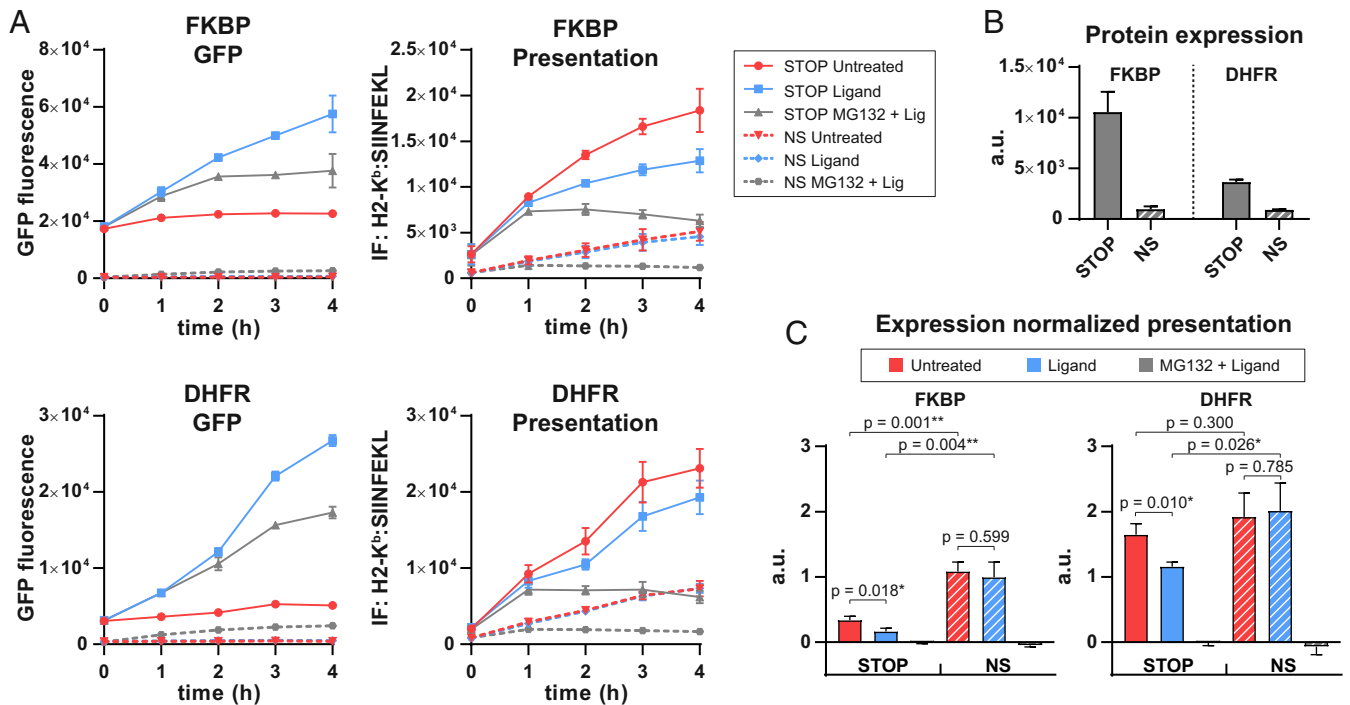


Fig. 2. Time course of antigen presentation from model STOP and NS proteins. (A) GFP fluorescence and presentation (immunolabeling fluorescence [IF] of surface H-2K^b:SIINFEKL complexes) levels in HeLa.K^b WT cells expressing the indicated NS and STOP proteins. At time 0, cells were stripped of immunopeptides by acid wash, followed by addition of DD ligand and/or proteasome inhibitor to the cell culture medium. (B) Estimated protein expression of each construct, based on the GFP accumulation in the presence of MG132+ligand during the first hour of treatment, that is, before onset of MG132-induced inhibition of translation. (C) The presentation rate (slope in the linear range of the assay, 1 to 3 h) of each construct was normalized to the respective expression rate (shown in B). All graphs show averages and SD (in arbitrary units) of three independent experiments. *P* values from two-sided *t* test are indicated. Asterisks highlight statistically significant changes, **P* < 0.05 and ***P* < 0.01.

quantitation by label-free liquid chromatography (LC)-MS/MS (Fig. 4A). In total, the analysis identified 3,658 peptides that could be mapped to 2,016 proteins (Dataset S1) (42). The majority of peptides were nine residues long, corresponding to the optimal size for MHC-I binding (SI Appendix, Fig. S4). Unbiased motif clustering of these peptides showed that the majority of sequences fit into three clusters whose consensus motifs closely match the binding patterns described for the MHC-I alleles present in HeLa.K^b cells (SI Appendix, Fig. S4). One hundred three peptides from 100 different proteins (~3% of the detected immunopeptidome and ~5% of presented proteins) were significantly (2- to 105-fold) more abundant in the WT cells than in Listerin-KO cells (Fig. 4B), and therefore represent proteins for which RQC contributes to antigen presentation. For the majority of these peptides (91%), the average level of presentation was higher in cKO cells than in Listerin-KO cells (Dataset S1) (42), despite incomplete complementation (SI Appendix, Fig. S5). Moreover, hierarchical clustering analysis showed that the datasets from Listerin-KO and cKO cells separate into different subclusters (Fig. 4C), confirming that the observed differences are caused by the deletion of Listerin.

RQC substrates are expected to include proteins lacking C-terminal portions, depending on the site of translational stalling. This implies that the C terminus of proteins might be underrepresented in the group of Listerin-dependent immunopeptides. Analysis of the localization of the identified peptides within their originating proteins showed that, when normalized to total protein length, peptide positions for Listerin-dependent and independent immunopeptides were not significantly different (two-sided Mann-Whitney *P* = 0.551) (SI Appendix, Fig. S6). However, the Listerin-dependent peptides tended to localize to the center of proteins, being depleted not only from the

C terminus, as might have been expected, but also from the N terminus (SI Appendix, Fig. S6).

To be able to distinguish between changes in presentation and changes in expression resulting from the absence of Listerin, we also measured the total proteome of the cell extracts used as input for the MHC-I immunoprecipitation. Overall, the changes in protein expression between WT and Listerin-KO cells were limited (SI Appendix, Fig. S7A and Dataset S2) (42), although some changes, albeit small, were statistically significant due to the high number of biological replicates employed in the experiment (SI Appendix, Fig. S7A and B). While the total proteome analysis did not identify any ubiquitin ligases with up-regulated expression, multiple subunits of the exosome RNA degradation machinery were more abundant in Listerin-KO cells (SI Appendix, Fig. S7B and Dataset S2) (42), suggesting a partial adaptation to the RQC defect. Normalization of immunopeptidome to proteome values demonstrated that, for the majority of immunopeptides, the changes in presentation were not caused by changes in protein expression (SI Appendix, Fig. S7C).

Further analysis of the group of proteins for which Listerin contributes to presentation provided insights into the role of RQC in antigen presentation. We first analyzed the Listerin targets for their degradation kinetics, by comparing our immunopeptidome results with earlier degradation profiling data from human epithelial cells by McShane et al. (43). According to this study, 47% of proteins follow an exponential degradation (ED) profile, where the degradation rate is constant over time (43). It is assumed that, for this class of proteins, the degradation rate is determined by the stability of the folded state (and other factors) rather than by limited efficiency of de novo folding or assembly. In contrast, a sizable number of proteins (9.4%) follow a non-ED (NED) profile. These proteins are more likely to be degraded in

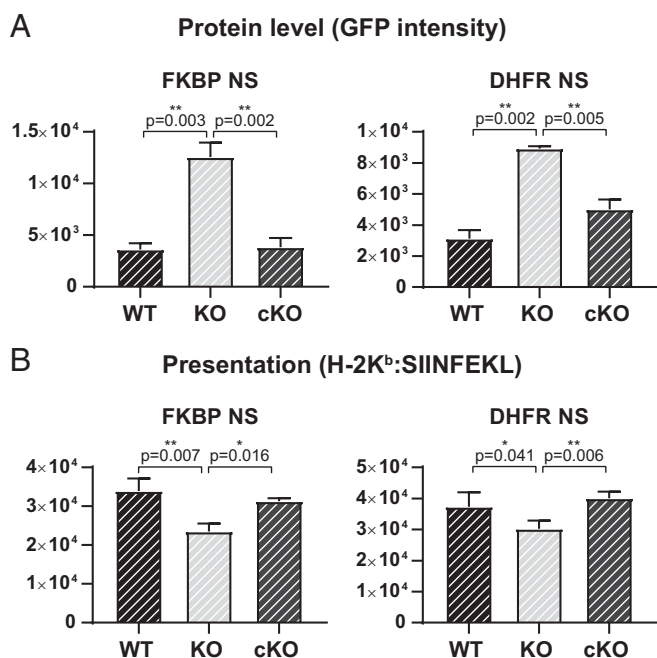


Fig. 3. Effect of Listerin on presentation of STOP and NS proteins. (A) Mean fluorescence intensity (in arbitrary units) of protein (GFP intensity) and (B) presentation (H-2K^b:SIINFEKL immunolabeling intensity) levels of NS proteins transiently transfected in the HeLa.K^b WT, Listerin-KO, and complemented cKO cell lines, in the presence of folding ligand. See *SI Appendix, Fig. S3* for representative flow cytometry plots and gating parameters. *P* values are from two-sided paired *t* test of three independent experiments. Asterisks highlight statistically significant changes, **P* < 0.05 and ***P* < 0.01.

the first hours after synthesis (Fig. 4 *D, Top*) (43). This suggests that proteins that follow NED have a lower chance of reaching their mature form, and are at an increased risk of being recognized as defective by the protein quality control machinery during folding and assembly. We found the antigenic peptides from proteins with ED to be slightly underrepresented in the immunopeptidome (41%) compared to the original dataset (47%, Fisher's exact test *P* = 0.0038), suggesting that they are more difficult to sample for antigen presentation (Fig. 4 *D, Bottom*). However, ED proteins were overrepresented in the group of Listerin targets, as compared to proteins with Listerin-independent presentation (57% vs. 40%, Fisher's exact test *P* = 0.053). In contrast, NED proteins tended to be less frequent among Listerin targets: While they represented 15% of Listerin-independent proteins, they accounted for only 6% of the Listerin targets (Fig. 4*D*). In conclusion, RQC degradation makes a measurable contribution to antigen presentation for proteins with exponential decay kinetics (ED proteins) that are characterized by efficient de novo folding and assembly. The ability of RQC to target such proteins may facilitate early sampling of viral proteins that have been evolutionarily selected for effective folding and high stability.

Insights into RQC Degradation. Multiple causes of ribosome stalling have been established, including premature polyadenylation of the mRNA, the presence of stable secondary structure, or long stretches of suboptimal codons in the mRNA (26, 29, 44–47). While these studies have been performed with model substrates, the endogenous targets of RQC degradation, and their underlying defects, remain largely unknown. Gene ontology (GO) enrichment analysis did not show any significant differences between the group of Listerin targets and the entire immunopeptidome dataset. In accordance, proteins with different cellular locations displayed similar WT/Listerin-KO immunopeptidome presentation

ratios (ANOVA *P* = 0.11; Fig. 5*A*). These observations highlight an important feature of RQC degradation—that it is not biased toward a specific molecular function, cellular component, or biological process. However, the Listerin targets identified by the immunopeptidome analysis were significantly larger in size than proteins with Listerin-independent presentation (median length of 623 and 513 amino acids, respectively, two-sided Mann–Whitney *P* = 0.024; *SI Appendix, Fig. S6B*). A possible explanation is that protein length correlates with mRNA complexity features, such as number of introns or secondary structure, which could render transcription and mRNA maturation more error-prone, and consequently more prone to ribosome stalling.

To gain insight into the natural causes for RQC degradation, we next asked whether the Listerin targets were more frequently subjected to premature mRNA polyadenylation, that is, the erroneous cleavage of the mRNA and poly(A) insertion within the coding sequence (internal polyadenylation), which leads to loss of the termination codon, poly(A) translation, and ribosomal stalling (35, 36). A quantitative measurement of poly(A) sites in transcripts of HeLa cells is provided by the PolyA_{DB} database (48, 49). Accordingly, the frequency of poly(A) sites inside the coding sequence tended to be higher among the Listerin targets than in the group of proteins where no effect of Listerin knockout on presentation was observed: 46% and 36%, respectively (Fig. 5*B*) (Fischer's exact test *P* = 0.072). Furthermore, the position of Listerin-dependent immunopeptides in the mRNA tended to be more frequently 5' relative to premature poly(A) site(s) than the position of Listerin-independent peptides (56% and 47%, respectively; Fig. 5*B*). Given the number of different RNA defects that have been demonstrated to cause ribosome stalling, one can predict the group of RQC substrates to be very heterogeneous. We therefore did not expect strong effects when analyzing traits correlating with the observed immunopeptidome changes. The fact that we could nonetheless observe an association of Listerin-dependent presentation with premature poly(A) sites supports the notion that internal polyadenylation is an important source of RQC substrates in vivo.

An interesting observation provided by the total proteome analysis of the HeLa.K^b Listerin-KO cell line was the GO term enrichment for “ER membrane protein complex” (EMC) and “mitochondrial outer membrane translocase complex” (TOM) among the up-regulated proteins in the Listerin-KO cells (*SI Appendix, Fig. S7B*). Of the nine detected EMC subunits, five showed a significant (*P* < 0.008) increase in protein abundance in the Listerin-KO cells. For the TOM complex, four out of the nine quantified subunits were increased (Fig. 5*C* and *Dataset S2*) (42). The EMC and TOM complexes have been implicated in the process of cotranslational insertion of transmembrane proteins into the ER and mitochondria, respectively (50–53). Prompted by this finding, we analyzed the proteins identified in the immunopeptidome for the presence of transmembrane domains (TMDs) using the Phobius transmembrane topology prediction server (54, 55). Transmembrane proteins in general (number of TMDs ≥ 1) were not overrepresented among the Listerin targets (Fig. 5*D*). However, there was a clear tendency for the enrichment of proteins with large numbers (>10) of TMDs: 4% of the Listerin targets versus 1.5% among proteins with Listerin-independent presentation (Fischer's exact test *P* = 0.073). In agreement, proteins with more than 10 TMDs displayed significantly higher WT/Listerin-KO immunopeptidome ratios than proteins not having any predicted TMD (Fig. 5*D*). Of note, proteins with >10 TMDs had also higher WT/Listerin-KO immunopeptidome ratios than randomly selected soluble (TMD *n* = 0) proteins of equal size (*SI Appendix, Fig. S8*). Thus, larger size alone does not explain the higher Listerin-dependent presentation of proteins with multiple TMDs. In conclusion, a high number of TMDs correlates with an increased propensity to undergo RQC degradation.

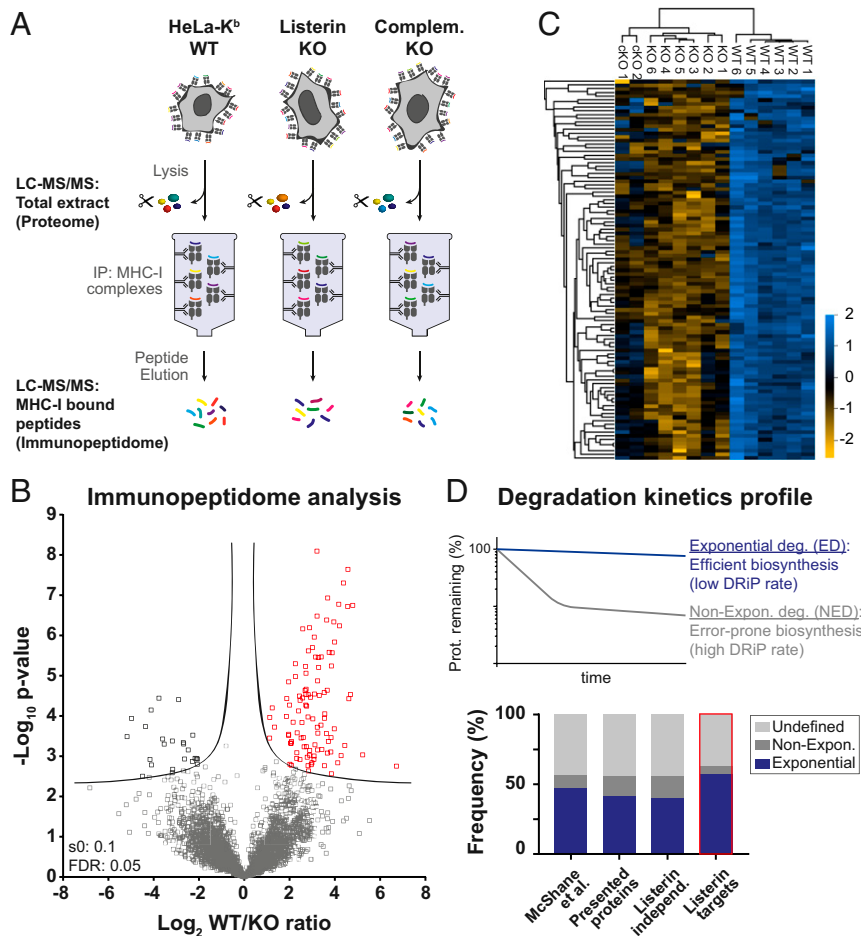


Fig. 4. Immunopeptidome analysis of HeLa.K^b WT and Listerin-KO cells. (A) General workflow of immunopeptidome analysis. After cell lysis, an aliquot of the total cell extract was digested with trypsin and used for total proteome analysis (Dataset S2 and SI Appendix, Fig. S7). The majority of the cell extract was submitted to immunoprecipitation of human and mouse MHC-I complexes. MHC-I-bound peptides were then eluted at low pH, followed by LC-MS/MS analysis. (B) Volcano plot showing changes in MHC-I-bound peptide abundance between WT and Listerin-KO cells. Peptides for which Listerin made a significant contribution to presentation (WT > KO, 103 peptides) are marked in red. (C) Hierarchical clustering analysis of Listerin-dependent peptides, including the cKO controls. Note that, due to partial rates of complementation (SI Appendix, Fig. S5), full WT levels were not reached in the cKO cells. (D) (Top) Diagram showing the characteristic decay profiles of exponentially (ED) and nonexponentially (NED) degraded proteins, according to McShane et al. (43). (Bottom) Frequency of different profiles of degradation kinetics (exponential, nonexponential, undefined) in groups of proteins with Listerin-dependent (highlighted with red outline) and independent presentation. Only proteins with available information on degradation kinetics (43) were considered (726 proteins of the 2,016 proteins characterized in the immunopeptidome analysis, 684 Listerin-independent and 35 Listerin-dependent targets).

Closer inspection of the group of Listerin targets revealed five proteins belonging to the solute carrier (SLC) family of membrane transport proteins (Fig. 5E). These proteins have 10 to 12 TMDs and no predicted N-terminal signal peptide sequence, and are annotated as being localized at the plasma membrane [although one of them, SLC41A3, has been reported to localize to the mitochondrial membrane (56)]. The EMC has been shown to be involved in the biogenesis of a range of multipass transmembrane proteins, with a particular enrichment for transporters (51). Thus, the Listerin-dependent representation of multipass membrane proteins in the immunopeptidome likely reflects a role of the RQC in quality control during the cotranslational insertion of such proteins into the ER and/or mitochondrial membranes.

Discussion

In this study, we have analyzed the capacity of the RQC machinery in producing epitopes for MHC class I-mediated antigen presentation. According to the DRiP hypothesis (7), antigen presentation relies on the fast degradation of newly synthesized proteins that fail to reach their structurally mature, functional

state. DRiPs can arise from deficiencies during protein translation, folding, and assembly (Fig. 6). Folding represents an intricate process requiring proteins to navigate a complex energy landscape, putting them at risk for adopting nonnative structures (57). Because misfolded proteins can form toxic aggregates, newly synthesized proteins are subjected to extensive scrutiny by quality control pathways that survey structural cues and target failed proteins to proteasomal degradation (Fig. 6). Folding errors are thought to be exploited by the adaptive immune system in generating antigenic peptides (11, 58). This implies that proteins having acquired highly efficient folding and maturation processes might evade presentation, including viral proteins that are under intense evolutionary pressure. Our results demonstrate that stalling during translation generates DRiPs whose degradation by the RQC pathway gives rise to efficient antigen presentation. RQC is unique in that degradation rates are largely independent of the folding state of its substrates, as shown here using NS protein constructs containing structurally unstable FKBP or DHFR domains. While addition of stabilizing ligand had only a minor effect on degradation and did not reduce presentation rates of these NS proteins, it significantly decreased both degradation

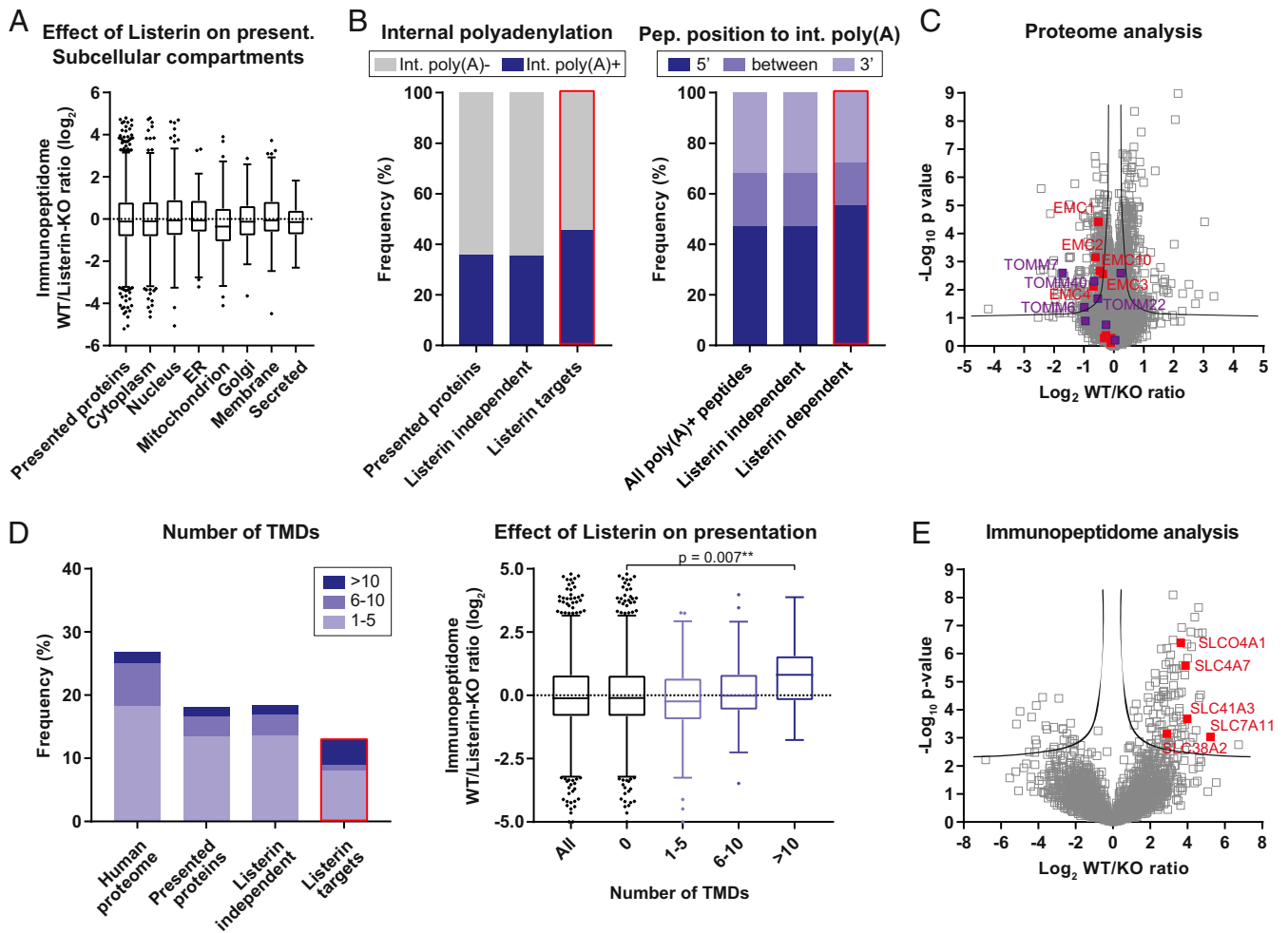


Fig. 5. Properties of proteins associated with RQC degradation and presentation. (A) WT/Listerin-KO averaged immunopeptide ratios for MHC-I presented proteins grouped according to their subcellular location annotated in Uniprot. (A and D) In the Tukey box plots, solid horizontal lines correspond to 25th to 75th percentiles and median value, whisker caps indicate 1.5 interquartile distance, and individual data points indicate outliers. (B) (Left) Frequency of proteins/genes having at least one detectable poly(A) site inside the protein coding sequence. Only proteins for which information was available in the poly(A)_DB were considered: 1,686 proteins with presented peptides, 1,597 Listerin-independent and 79 Listerin targets (red outline). (Right) Frequency of immunopeptides classified according to their localization in the mRNA in relation to internal polyadenylation site(s): 5' to all poly(A) site(s), between (peptide is localized in between the first and the last internal poly(A), in cases where multiple internal sites have been identified for the same gene), and 3' (peptide is encoded 3' to all internal poly(A) site(s)). Only peptides mapped to internal polyadenylation-containing genes (according to the polyA_DB) were considered: 1,451 peptides in total, 1,412 Listerin-independent and 36 Listerin-dependent (red outline). (C) Total proteome analysis of Listerin-KO cells (as in *SI Appendix*, Fig. S7) with EMC and TOM complex proteins highlighted in red and purple, respectively. The subunits significantly increased in the KO cells are labeled. (D) (Left) Frequency of proteins with different numbers of TMDs, according to the Phobius predictor. (Right) Averaged immunopeptide WT/KO ratios of proteins grouped according to the number of TMDs. *P* value: ANOVA with Dunnett test in relation to TMD = 0. ANOVA test for trend also shows higher tendency for Listerin effect in groups with increasing number of TMDs (left to right groups, *P* = 0.0015). (E) Immunopeptide results (as in Fig. 4B), with Listerin-dependent peptides derived from multispanning membrane proteins marked in red. The corresponding gene names are indicated. Asterisks highlight statistically significant changes, **P* < 0.05 and ***P* < 0.01.

and presentation of the corresponding STOP proteins. Thus, the RQC pathway could be particularly important in antigen presentation from proteins that circumvent folding-dependent quality control due to their efficient folding and maturation properties (Fig. 6).

Because RQC degradation occurs very early in protein biosynthesis (Fig. 6), it allows fast sampling for antigen presentation. Kinetic analysis of presentation showed that, for proteins reaching a stably folded state (in the presence of ligand), the presentation rate obtained for RQC-mediated degradation (NS protein) can be sixfold higher than presentation obtained from its intrinsic synthesis error and turnover (STOP protein). Strikingly, even for a folding-compromised protein, such as FKBP STOP in the absence of ligand, RQC can still result in an approximately threefold faster

presentation rate, reflecting a major kinetic advantage of RQC over posttranslational quality control (Fig. 6).

Our immunopeptide analysis of Listerin-deficient cells showed that RQC indeed contributes to the MHC-I repertoire. We identified 103 peptides with significantly reduced presentation (2- to 105-fold) in the absence of Listerin. These peptides represent a relatively small (~3%) fraction of the quantified dataset. However, our experiments with model proteins (Fig. 1) indicate that Listerin is not the only ubiquitin ligase responsible for degradation of ribosome-stalled nascent chains. Moreover, the total proteome analysis of Listerin-KO cells showed an up-regulation of RNA degradation machinery, which may reduce the amount of RQC substrates. For these reasons, our analysis is likely to underestimate the contribution of RQC to antigen presentation.

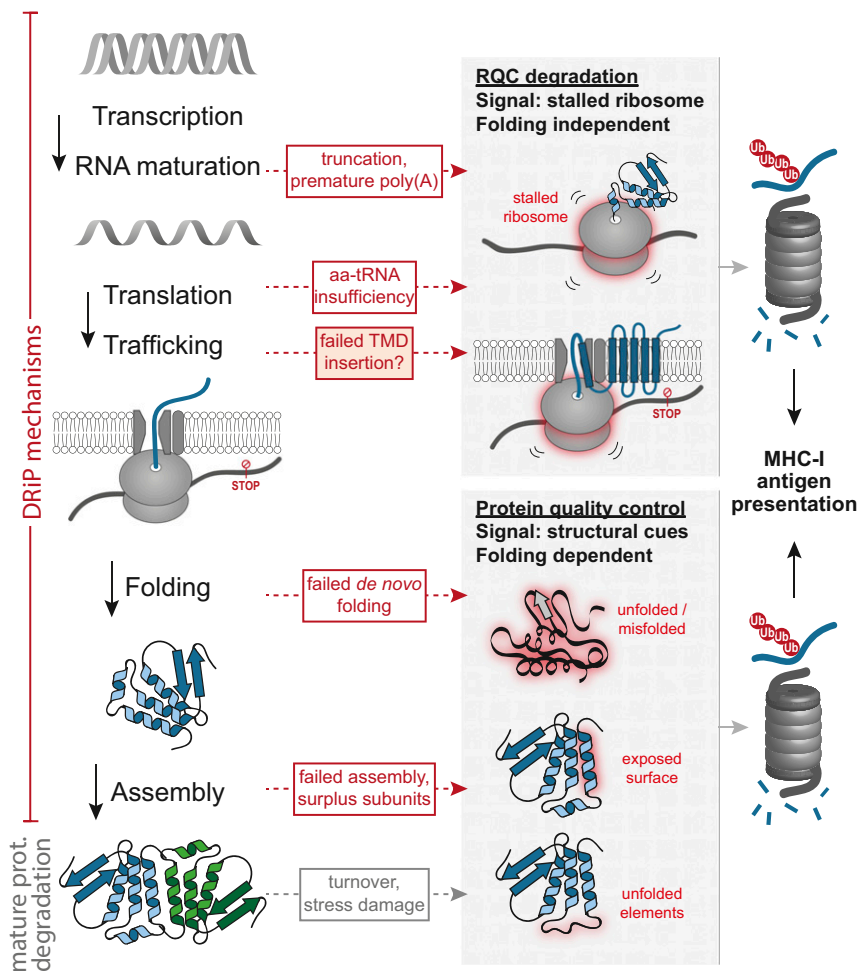


Fig. 6. MHC-I antigen presentation during protein synthesis and turnover. The process of protein biosynthesis (left column) leading to stable, functional protein comprises multiple steps. Errors may result in DRIPs, which are targeted for ubiquitin-dependent proteasomal degradation and therefore can sample newly synthesized proteins for antigen presentation. The RQC pathway (top gray panel) functions to degrade stalled polypeptide chains in a manner independent of their folding state. This situation mainly arises from errors in mRNA synthesis and maturation. Our results suggest that failed cotranslational insertion into membranes of proteins with multiple transmembrane segments also causes stalling and triggers RQC-mediated degradation. Folding-dependent protein quality control pathways survey structural cues to identify errors in protein folding and assembly as well as mature protein damage (lower gray panel).

Nevertheless, the immunopeptidome results provide support for the prediction that RQC is preferentially important for improving the presentation of proteins that have a high propensity to reach a folded mature state (identified here as proteins with ED).

As MHC-I presentation should reflect proteasomal degradation, the immunopeptidome can be used as a powerful screening tool for RQC substrates. Limitations of this approach include the dilution of the RQC effect for proteins that are highly degraded by other pathways, and the possibility that certain truncated RQC substrates might lack immunogenic peptides. Notably, our data support a role of premature polyadenylation in generating endogenous RQC substrates, consistent with current understanding (49, 59, 60). Interestingly, our analysis also identified several multipass transmembrane proteins as RQC substrates, along with an up-regulation of the EMC and TOM membrane insertion machineries in RQC-deficient cells. A recent study mapping EMC substrates by proximity-specific ribosome profiling reported that EMC binds to proteins whose ER membrane insertion represents a challenge due to the high number of TMDs and/or the presence of charged residues in the membrane-spanning segments (51). These are structural features shared by the members of the SLC family of

transport proteins we identified as Listerin targets. It seems plausible, therefore, that the up-regulation of membrane insertion machinery is an adaptation to the presence of insertion-stalled SLC (and other TMD) proteins in Listerin-deficient cells. Indeed, it is known that Listerin can ubiquitylate nascent polypeptides stalled at the Sec61 translocon of the ER membrane (61, 62). In principle, ribosome stalling during membrane translocation could be triggered by the same mRNA defects engaging the RQC in the cytosol (61). However, proteins with low numbers of TMD domains (and secretory proteins in general) were not identified as preferential RQC substrates. This suggests that stalling in the case of the SLC proteins takes place as a result of the difficult-to-insert nature of these multipass proteins, rather than due to mRNA defects. Assuming a link between membrane translocation and ribosomal elongation, improper membrane insertion could result in stalling of the membrane-anchored ribosome, in turn leading to ribosome collision, a trigger of RQC recruitment (49). This mechanism would ensure degradation of substrates that might otherwise escape ERAD, as in the case of truncated proteins that acquire sufficient folding (61). Another possibility is that the mRNAs encoding multispansing transmembrane proteins represent targets of regulated Ire1-dependent decay (63, 64). In order to decrease

the burden of ER protein synthesis during stress situations, Ire1 cleaves ER-localized mRNAs at specific sites within the coding sequence. This results in mRNA species lacking stop codons and poly(A) tails (65), which are likely to cause ribosome stalling.

It is noteworthy, in this context, that flaviviruses such as Zika and Dengue translate their genome into a single multipass transmembrane protein at the ER, which is later cleaved into 10 different proteins (66). Accordingly, these viruses were shown to require the EMC during the early stages of replication (67, 68). The observed trend for multipass transmembrane proteins among RQC substrates may thus facilitate the early detection of these viral infections.

Materials and Methods

Purification of MHC-I Peptides. Immunopeptidome analysis was performed with six large independent cultures of HeLa.K^b WT and Listerin-KO, and two cultures of the stably complemented KO control cell line. Cells were grown in Nunc Cell Factory Systems (Thermo Scientific) of 2,528 cm² culture surface. After reaching a semiconfluent state, cells were harvested with TrypLE Express Enzyme and washed twice in phosphate-buffered saline (PBS), and dry pellets were flash frozen and stored at -80 °C until further use. The yields per culture ranged from 2.9 × 10⁸ to 4.3 × 10⁸ cells (3.7 × 10⁸ on average). MHC-I complex immunoprecipitation and peptide ligand purification were performed as previously described (69). Briefly, cell pellets were resuspended in 8 mL of PBS with 0.25% sodium deoxycholate (Sigma-Aldrich), 1% octyl-β-D glucopyranoside (Sigma-Aldrich), 0.2 mM iodoacetamide, 1 mM (ethylenedinitrilo) tetraacetic acid, and 1:200 Protease Inhibitor Mixture (Sigma-Aldrich) and lysed at 4 °C for 1 h. The lysates were then cleared by centrifugation at 40,000 × g at

4 °C for 30 min. MHC-I immunoprecipitation was performed on the cleared lysate with 2 mg of the panHLA-I antibody W6/32 (purified from HB95 cells; ATCC) covalently bound to protein-A Sepharose beads (Invitrogen), and MHC-I complexes were eluted at room temperature with 0.1 N acetic acid. The eluted molecules were then loaded on Sep-Pak tC18 cartridges (Waters), and the MHC-I peptides were separated from the MHC-I complexes by eluting them with 30% acetonitrile (ACN) in 0.1% trifluoroacetic acid (TFA). Peptides were then further purified using Silica C-18 column tips (Harvard Apparatus), eluted again with 30% ACN in 0.1% TFA, and concentrated by vacuum centrifugation. Finally, MHC-I peptides were resuspended with 2% ACN in 0.1% TFA for single-shot LC-MS/MS analysis. Additional experimental procedures are described in *SI Appendix*.

Data Availability. All data are contained in the main text, *SI Appendix*, or *Datasets S1* and *S2*. The MS proteomics data have been deposited to the ProteomeXchange Consortium via the PRIDE (70) partner repository with the dataset identifier PXD014644. Any further details are available upon request.

ACKNOWLEDGMENTS. This project has received funding from the European Union's Horizon 2020 research and innovation program under the Marie Skłodowska-Curie Grant Agreement 749932, and from the European Commission 7th Research Framework Program Grant GA ERC-2012-SyG_318987-TopAG. We thank Amgen scholar Evi Zhuleku for conducting protein synthesis experiments; Mi-Jeong Yoon and Young Jun Choe for sharing Listerin knockout and overexpression plasmids; and Martin Spitaler and Markus Oster from the Imaging Facility of the Max Planck Institute of Biochemistry for assistance with cell sorting and flow cytometry analysis. We are grateful to Prof. Kenneth L. Rock for providing the HeLa.K^b cell line.

1. K. L. Rock, A. L. Goldberg, Degradation of cell proteins and the generation of MHC class I-presented peptides. *Annu. Rev. Immunol.* **17**, 739–779 (1999).
2. K. L. Rock *et al.*, Inhibitors of the proteasome block the degradation of most cell proteins and the generation of peptides presented on MHC class I molecules. *Cell* **78**, 761–771 (1994).
3. V. Cohen-Kaplan, I. Livneh, N. Avni, C. Cohen-Rosenzweig, A. Ciechanover, The ubiquitin-proteasome system and autophagy: Coordinated and independent activities. *Int. J. Biochem. Cell Biol.* **79**, 403–418 (2016).
4. A. Varshavsky, The ubiquitin system, autophagy, and regulated protein degradation. *Annu. Rev. Biochem.* **86**, 123–128 (2017).
5. F. Esquivel, J. Yewdell, J. Bennink, RMA/S cells present endogenously synthesized cytosolic proteins to class I-restricted cytotoxic T lymphocytes. *J. Exp. Med.* **175**, 163–168 (1992).
6. J. W. Yewdell, DRiPs solidify: Progress in understanding endogenous MHC class I antigen processing. *Trends Immunol.* **32**, 548–558 (2011).
7. J. W. Yewdell, L. C. Antón, J. R. Bennink, Defective ribosomal products (DRiPs): A major source of antigenic peptides for MHC class I molecules? *J. Immunol.* **157**, 1823–1826 (1996).
8. J. Yewdell, To DRiP or not to DRiP: Generating peptide ligands for MHC class I molecules from biosynthesized proteins. *Mol. Immunol.* **39**, 139–146 (2002).
9. U. Schubert *et al.*, Rapid degradation of a large fraction of newly synthesized proteins by proteasomes. *Nature* **404**, 770–774 (2000).
10. R. M. Vabulas, F. U. Hartl, Protein synthesis upon acute nutrient restriction relies on proteasome function. *Science* **310**, 1960–1963 (2005).
11. K. L. Rock, D. J. Farfán-Arribas, J. D. Colbert, A. L. Goldberg, Re-examining class-I presentation and the DRiP hypothesis. *Trends Immunol.* **35**, 144–152 (2014).
12. L. C. Antón, J. W. Yewdell, Translating DRiPs: MHC class I immunosurveillance of pathogens and tumors. *J. Leukoc. Biol.* **95**, 551–562 (2014).
13. S. Duttler, S. Pechmann, J. Frydman, Principles of cotranslational ubiquitination and quality control at the ribosome. *Mol. Cell* **50**, 379–393 (2013).
14. B. P. Dolan, J. R. Bennink, J. W. Yewdell, Translating DRiPs: Progress in understanding viral and cellular sources of MHC class I peptide ligands. *Cell. Mol. Life Sci.* **68**, 1481–1489 (2011).
15. S.-B. Qian *et al.*, Tight linkage between translation and MHC class I peptide ligand generation implies specialized antigen processing for defective ribosomal products. *J. Immunol.* **177**, 227–233 (2006).
16. B. P. Dolan *et al.*, Distinct pathways generate peptides from defective ribosomal products for CD8+ T cell immunosurveillance. *J. Immunol.* **186**, 2065–2072 (2011).
17. B. M. Fiebigler, A. Moosmann, U. Behrends, J. Mautner, Mature proteins derived from Epstein-Barr virus fail to feed into the MHC class I antigenic pool. *Eur. J. Immunol.* **42**, 3167–3173 (2012).
18. S. Khan *et al.*, Cutting edge: Neosynthesis is required for the presentation of a T cell epitope from a long-lived viral protein. *J. Immunol.* **167**, 4801–4804 (2001).
19. J. D. Colbert, D. J. Farfán-Arribas, K. L. Rock, Substrate-induced protein stabilization reveals a predominant contribution from mature proteins to peptides presented on MHC class I. *J. Immunol.* **191**, 5410–5419 (2013).
20. D. J. Farfán-Arribas, L. J. Stern, K. L. Rock, Using intein catalysis to probe the origin of major histocompatibility complex class I-presented peptides. *Proc. Natl. Acad. Sci. U.S.A.* **109**, 16998–17003 (2012).
21. O. Brandman *et al.*, A ribosome-bound quality control complex triggers degradation of nascent peptides and signals translation stress. *Cell* **151**, 1042–1054 (2012).
22. O. Brandman, R. S. Hegde, Ribosome-associated protein quality control. *Nat. Struct. Mol. Biol.* **23**, 7–15 (2016).
23. J. Chu *et al.*, A mouse forward genetics screen identifies LISTERIN as an E3 ubiquitin ligase involved in neurodegeneration. *Proc. Natl. Acad. Sci. U.S.A.* **106**, 2097–2103 (2009).
24. Q. Defenouillère *et al.*, Cdc48-associated complex bound to 60S particles is required for the clearance of aberrant translation products. *Proc. Natl. Acad. Sci. U.S.A.* **110**, 5046–5051 (2013).
25. D. Lyumkis *et al.*, Structural basis for translational surveillance by the large ribosomal subunit-associated protein quality control complex. *Proc. Natl. Acad. Sci. U.S.A.* **111**, 15981–15986 (2014).
26. M. H. Bengtson, C. A. P. Joazeiro, Role of a ribosome-associated E3 ubiquitin ligase in protein quality control. *Nature* **467**, 470–473 (2010).
27. K. K. Kostova *et al.*, CAT-tailing as a fail-safe mechanism for efficient degradation of stalled nascent polypeptides. *Science* **357**, 414–417 (2017).
28. P. A. Frischmeyer *et al.*, An mRNA surveillance mechanism that eliminates transcripts lacking termination codons. *Science* **295**, 2258–2261 (2002).
29. M. K. Doma, R. Parker, Endonucleolytic cleavage of eukaryotic mRNAs with stalls in translation elongation. *Nature* **440**, 561–564 (2006).
30. R. Rakhit, R. Navarro, T. J. Wandless, Chemical biology strategies for posttranslational control of protein function. *Chem. Biol.* **21**, 1238–1252 (2014).
31. E. L. Egeler, L. M. Urner, R. Rakhit, C. W. Liu, T. J. Wandless, Ligand-switchable substrates for a ubiquitin-proteasome system. *J. Biol. Chem.* **286**, 31328–31336 (2011).
32. L. A. Banaszynski, L. C. Chen, L. A. Maynard-Smith, A. G. L. Ooi, T. J. Wandless, A rapid, reversible, and tunable method to regulate protein function in living cells using synthetic small molecules. *Cell* **126**, 995–1004 (2006).
33. M. Iwamoto, T. Björklund, C. Lundberg, D. Kirik, T. J. Wandless, A general chemical method to regulate protein stability in the mammalian central nervous system. *Chem. Biol.* **17**, 981–988 (2010).
34. A. Porgador, J. W. Yewdell, Y. Deng, J. R. Bennink, R. N. Germain, Localization, quantitation, and in situ detection of specific peptide-MHC class I complexes using a monoclonal antibody. *Immunity* **6**, 715–726 (1997).
35. L. Arthur *et al.*, Translational control by lysine-encoding A-rich sequences. *Sci. Adv.* **1**, e1500154 (2015).
36. S. Juszkiewicz, R. S. Hegde, Initiation of quality control during poly(A) translation requires site-specific ribosome ubiquitination. *Mol. Cell* **65**, 743–750.e4 (2017).
37. I. A. York *et al.*, The ER aminopeptidase ERAP1 enhances or limits antigen presentation by trimming epitopes to 8–9 residues. *Nat. Immunol.* **3**, 1177–1184 (2002).
38. H. Y. Jiang, R. C. Wek, Phosphorylation of the alpha-subunit of the eukaryotic initiation factor-2 (eIF2alpha) reduces protein synthesis and enhances apoptosis in response to proteasome inhibition. *J. Biol. Chem.* **280**, 14189–14202 (2005).
39. C. S. Sitron, O. Brandman, CAT tails drive degradation of stalled polypeptides on and off the ribosome. *Nat. Struct. Mol. Biol.* **26**, 450–459 (2019).
40. S. Sugawara, T. Abo, K. Kumagai, A simple method to eliminate the antigenicity of surface class I MHC molecules from the membrane of viable cells by acid treatment at pH 3. *J. Immunol. Methods* **100**, 83–90 (1987).
41. A. van Hoof, P. A. Frischmeyer, H. C. Dietz, R. Parker, Exosome-mediated recognition and degradation of mRNAs lacking a termination codon. *Science* **295**, 2262–2264 (2002).

42. D. B. Trentini *et al.*, Role for ribosomal quality control in sampling proteins for MHC class I-mediated antigen presentation. ProteomeXchange. <http://www.ebi.ac.uk/pride/archive/projects/PXD014644>. Deposited 17 July 2019.
43. E. McShane *et al.*, Kinetic analysis of protein stability reveals age-dependent degradation. *Cell* **167**, 803–815.e21 (2016).
44. T. Tsuboi *et al.*, Dom34:hbs1 plays a general role in quality-control systems by dissociation of a stalled ribosome at the 3' end of aberrant mRNA. *Mol. Cell* **46**, 518–529 (2012).
45. D. P. Letzring, A. S. Wolf, C. E. Brule, E. J. Grayhack, Translation of CGA codon repeats in yeast involves quality control components and ribosomal protein L1. *RNA* **19**, 1208–1217 (2013).
46. K. Ikeuchi, T. Inada, Ribosome-associated Asc1/RACK1 is required for endonucleolytic cleavage induced by stalled ribosome at the 3' end of nonstop mRNA. *Sci. Rep.* **6**, 28234 (2016).
47. S. Ito-Harashima, K. Kuroha, T. Tatematsu, T. Inada, Translation of the poly(A) tail plays crucial roles in nonstop mRNA surveillance via translation repression and protein destabilization by proteasome in yeast. *Genes Dev.* **21**, 519–524 (2007).
48. R. Wang, D. Zheng, G. Yehia, B. Tian, A compendium of conserved cleavage and polyadenylation events in mammalian genes. *Genome Res.* **28**, 1427–1441 (2018).
49. S. Juskiewicz *et al.*, ZNF598 is a quality control sensor of collided ribosomes. *Mol. Cell* **72**, 469–481.e7 (2018).
50. P. J. Chitwood, S. Juskiewicz, A. Guna, S. Shao, R. S. Hegde, EMC is required to initiate accurate membrane protein topogenesis. *Cell* **175**, 1507–1519.e16 (2018).
51. M. J. Shurtleff *et al.*, The ER membrane protein complex interacts cotranslationally to enable biogenesis of multipass membrane proteins. *eLife* **7**, e37018 (2018).
52. C. C. Williams, C. H. Jan, J. S. Weissman, Targeting and plasticity of mitochondrial proteins revealed by proximity-specific ribosome profiling. *Science* **346**, 748–751 (2014).
53. M. Bohnert, N. Pfanner, M. van der Laan, Mitochondrial machineries for insertion of membrane proteins. *Curr. Opin. Struct. Biol.* **33**, 92–102 (2015).
54. L. Käll, A. Krogh, E. L. L. Sonnhammer, Advantages of combined transmembrane topology and signal peptide prediction—The Phobius web server. *Nucleic Acids Res.* **35** (suppl. 2), W429–W432 (2007).
55. L. Käll, A. Krogh, E. L. L. Sonnhammer, A combined transmembrane topology and signal peptide prediction method. *J. Mol. Biol.* **338**, 1027–1036 (2004).
56. L. Mastrototaro, A. Smorodchenko, J. R. Aschenbach, M. Kolisek, G. Sponder, Solute carrier 41A3 encodes for a mitochondrial Mg²⁺ efflux system. *Sci. Rep.* **6**, 27999 (2016).
57. D. Balchin, M. Hayer-Hartl, F. U. Hartl, In vivo aspects of protein folding and quality control. *Science* **353**, aac4354 (2016).
58. J. W. Yewdell, E. Reits, J. Neefjes, Making sense of mass destruction: Quantitating MHC class I antigen presentation. *Nat. Rev. Immunol.* **3**, 952–961 (2003).
59. A. Garzia *et al.*, The E3 ubiquitin ligase and RNA-binding protein ZNF598 orchestrates ribosome quality control of premature polyadenylated mRNAs. *Nat. Commun.* **8**, 16056 (2017).
60. C. A. P. Joazeiro, Ribosomal stalling during translation: Providing substrates for ribosome-associated protein quality control. *Annu. Rev. Cell Dev. Biol.* **33**, 343–368 (2017).
61. K. von der Malsburg, S. Shao, R. S. Hegde, The ribosome quality control pathway can access nascent polypeptides stalled at the Sec61 translocon. *Mol. Biol. Cell* **26**, 2168–2180 (2015).
62. S. Arakawa *et al.*, Quality control of nonstop membrane proteins at the ER membrane and in the cytosol. *Sci. Rep.* **6**, 30795 (2016).
63. J. Hollien *et al.*, Regulated Ire1-dependent decay of messenger RNAs in mammalian cells. *J. Cell Biol.* **186**, 323–331 (2009).
64. J. Hollien, J. S. Weissman, Decay of endoplasmic reticulum-localized mRNAs during the unfolded protein response. *Science* **313**, 104–107 (2006).
65. N. R. Guydosh, P. Kimmig, P. Walter, R. Green, Regulated Ire1-dependent mRNA decay requires no-go mRNA degradation to maintain endoplasmic reticulum homeostasis in *S. pombe*. *eLife* **6**, e29216 (2017).
66. S. S. Hasan, M. Sevvana, R. J. Kuhn, M. G. Rossmann, Structural biology of Zika virus and other flaviviruses. *Nat. Struct. Mol. Biol.* **25**, 13–20 (2018).
67. G. Savidis *et al.*, Identification of Zika virus and Dengue virus dependency factors using functional genomics. *Cell Rep.* **16**, 232–246 (2016).
68. D. L. Lin *et al.*, The ER membrane protein complex promotes biogenesis of Dengue and Zika virus non-structural multi-pass transmembrane proteins to support infection. *Cell Rep.* **27**, 1666–1674.e4 (2019).
69. M. Bassani-Sternberg, S. Pletscher-Frankild, L. J. Jensen, M. Mann, Mass spectrometry of human leukocyte antigen class I peptidomes reveals strong effects of protein abundance and turnover on antigen presentation. *Mol. Cell. Proteomics* **14**, 658–673 (2015).
70. Y. Perez-Riverol *et al.*, The PRIDE database and related tools and resources in 2019: Improving support for quantification data. *Nucleic Acids Res.* **47**, D442–D450 (2019).